Review

High Performance Photopyroelectric Calorimetry of Liquids

Dorin Dadarlat* and Camelia Neamtu

National R&D Institute for Isotopic and Molecular Technologies,
No. 65-103 Donath Street, POB 700, 400293 Cluj-Napoca, Romania

**Corresponding author: E-mail: dadarlat@itim-cj.ro*
Phone: +40 264 584037; fax: +40 264 420042

Received: 15-07-2008

Abstract

A review of the main photopyroelectric (PPE) calorimetric techniques proposed in the last years for accurate measurements of dynamic thermal parameters (thermal effusivity and thermal diffusivity) of liquids is presented. The possibilities offered by the two PPE detection configurations ("back" and "front") are analyzed, and the information contained in the amplitude and phase of the PPE signal are compared. A study of the accuracy of the investigations when using the frequency or thickness scan method is also made. Some basic applications concerning high-resolution measurements of thermal diffusivity and effusivity of some "special" liquid samples (isotopic liquid mixtures, magnetic nanofluids, liquid foodstuffs) are described.

Keywords: Photothermal phenomena, photopyroelectric calorimetry, dynamic thermal parameters, liquids

1. Introduction

The photopyroelectric (PPE) detection was introduced in 1984, as a powerful tool for high resolution measurement of thermal properties of materials.[1–3] In principle, in the PPE method the temperature variation of a sample, exposed to a modulated radiation, is measured with a pyroelectric sensor, situated in intimate thermal contact with the sample.[4, 5]

In the most general case, the complex PPE signal depends on all optical and thermal parameters of the layers of the detection cell (usually six: air, window, sample, pyroelectric sensor, substrate and backing). A large effort was dedicated in the last decades to simplify the mathematical expression of the PPE signal, by acting especially on the number of components of the detection cell and on the thermal and optical thickness of each layer. As a final result, several particular cases were obtained, in which the information is contained both in the amplitude and phase of the PPE signal;[4–6] the amplitude and phase depend in these cases on one or, in a simple way, on two of the sample's related thermal parameters.

The thermal parameters resulting directly from PPE measurements are usually the "fundamental" ones (present in the thermal diffusion equation and its solution): the thermal diffusivity and effusivity. It is well known that the four thermal parameters, the static volume specific heat, C, and the dynamic thermal diffusivity, α, conductivity, k, and effusivity, e, are connected by two relationships, $k = C\,\alpha$ and $e = (C\,k)^{1/2}$; in conclusion only two are independent.

Concerning the PPE detection configurations, two of them, "back" and "front" respectively, have been mainly applied for calorimetric purposes.

In the back (standard) configuration, a modulated light impinges on the front surface of a sample, and a pyroelectric sensor, situated in good thermal contact with the sample's rear side, measures the heat developed in the sample due to the absorption of radiation.[6, 7] In the front (inverse) configuration, the radiation impinges on the front surface of the sensor, and the sample, in good thermal contact with its rear side, acts as a heat sink.[8, 9]

Even if the PPE method can be successfully applied to gases, liquids and solids, we restrict, in this paper, the area of interest only to liquids, because the sample-sensor thermal contact is in this case perfect, leading to accurate quantitative results. For solid samples, the sample-sensor coupling fluid (always necessary) can bring uncontrolled

errors. Concerning gases, the PPE calorimetry can be also used, but in very special conditions, due to the low optical absorption coefficients of gases and to large thermal diffusion lengths.

Historically speaking, the PPE calorimetry developed many ways in order to obtain the values of the thermal parameters. Some of them are based on the measurement of single values;[8, 10] other alternatives make use of scanning procedures.[11] The second type of investigations is proved to be more precise. When liquid samples are investigated, there are two parameters susceptible to be scanned: the chopping frequency of incident radiation and the sample's thickness.

In principle, any combination detection configuration (*back* or *front*) – source of information (PPE *amplitude* or *phase*) – scanning parameter (chopping *frequency* or sample's *thickness* scan) is possible, in order to obtain one of the dynamic thermal parameters (thermal *diffusivity* or *effusivity*). The paper is in fact a review of all these possible combinations, stressing on the recent developed ones with the purpose of high accuracy measurements.

2. Theory

In this theoretical section we will present the mathematical equations of the complex PPE signal used in the two detection configurations. It is now well known that the general expression for the PPE signal is analytically exact,[4, 5] but it is too complicated for experimental applications. Several assumptions have to be made from the beginning, to simplify it. These assumptions have a general character and it is very easy to set-up them experimentally. They are: *(i)* a one dimensional propagation of heat is considered; *(ii)* the heat transport is due only to the conduction (the heat transport by radiation and convection is neglected). This second assumption is justified in the paper by the relatively small samples' thickness. When large cavity lengths are involved, the thermal-wave radiation power transfer becomes dominant.[11, 14]

Additional restrictions will be imposed in each particular case.

2. 1. Back Configuration

The geometry of the back PPE configuration is presented in Fig. 1.[12]

With the additional simplifying assumptions, that is the window and substrate are thermally thick, the air and window are optically transparent and the incident radiation is absorbed at the window-material interface (by a thin opaque layer), the PPE voltage is given by:[12]

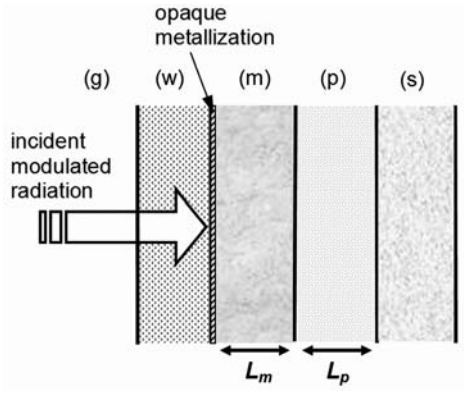

Figure 1. Schematic diagram of the PPE detection cell: (g) – air, (w) – window, (m) – material, (p) – pyroelectric sensor, (s) – substrate.

where

$$R_{jk} = (b_{jk} - 1)/(b_{jk} + 1); \quad b_{jk} = e_j / e_k ; \qquad \sigma_j = (1 + i)a_j ; \ \mu = (2\alpha/\omega)^{1/2} \tag{2}$$

In Eq. (1) V_0 is an instrumental factor, R_{jk} represents the reflection coefficient of the thermal wave at the '*jk*' interface, ω is the angular chopping frequency and σ and a are the complex thermal diffusion coefficient and the reciprocal of the thermal diffusion length ($a = 1/\mu$), respectively.

In order to eliminate V_0, a normalization of the signal is necessary, the best reference signal being obtained by the direct illumination of the empty sensor. If, additionally, we work in the thermally thick regime for the sensor ($L_p >> \mu_p$) and we extract the phase and the amplitude from Eq. (1), we get for the phase:

$$\Theta = -\arctan \frac{\tan(a_m L_m)\left[1 + R\, e^{-2a_m L_m}\right]}{1 - R\, e^{-2a_m L_m}} \tag{3}$$

with $R = R_{mw} R_{mp}$, and for the amplitude:

$$\ln |V_n| = \ln \frac{2(b_{gp} + 1)}{(b_{wm} + 1)(b_{mp} + 1)} - a_m L_m \tag{4}$$

An analysis of Eq. (3) indicates that the sample's thermal diffusivity (contained in a_m) can be directly measured by performing a frequency and/or a sample's thickness scan of the phase of the PPE signal. The most suitable particular case seems to be the thermally thick regime for the sample, ($L_m >> \mu_m$), when Eq.(3) reduces to:

$$\Theta = \Theta_0 - L_m \left(\frac{\omega}{2\alpha_m} \right)^{1/2} \tag{5}$$

$$V = \frac{2V_0 e^{-\sigma_m L_m}}{(b_{wm}+1)(b_{mp}+1)} \frac{e^{\sigma_p L_p} + R_{sp} e^{-\sigma_p L_p} - (1 + R_{sp})}{e^{\sigma_p L_p} - R_{sp} R_{mp} e^{-\sigma_p L_p} + (R_{mp} e^{\sigma_p L_p} - R_{sp} e^{-\sigma_p L_p}) R_{wm} e^{-2\sigma_m L_m}} \tag{1}$$

At this stage, there are two ways to deduce the thermal diffusivity. The first one is to use the slope of the curves $\Theta = \Theta(f^{1/2})$ or $\Theta = \Theta(L_m)$. This method is a direct one, and involves no calibration. Historically, the frequency scan was mainly used in the past, probably due to the fact that it could be applied both to solid and liquid samples. Relative errors lying between ±2% and ±5% (depending on the frequency range) obtained with this method, are reported.[12] However, sometimes, when accurate measurements are necessary, the exact knowledge of the sample's thickness can be a problem, especially in the case of liquids. This is why methods based on a variable sample-to-source distance (so called thermal-wave resonator cavity, TWRC) were introduced.[11, 13–19] In such a method the chopping frequency is kept constant, and a sample's thickness scan of the phase is performed. The advantage of the method consists in the fact that the data processing does not need the exact knowledge of the sample's thickness, but only the sample's thickness variation. Typical relative errors obtained with this method are between ±0.8% and ±3%.[19,20]

In order to improve the accuracy of the results, Dadarlat et al.[20, 21] proposed an alternative of the TWRC method, based on the exact determination of the absolute values of phase of the signal and sample's thickness. The relationship used in this case to calculate the thermal diffusivity is:

$$\alpha_m = \frac{\pi f L_{\mathrm{mabs}}^{\ 2}}{\Theta_{\mathrm{abs}}^{\ 2}} \tag{6}$$

where Θ_{abs} and L_{mabs} are the absolute values of the PPE phase and sample's thickness.

The proposed way to find the correct value of the thermal diffusivity is in fact a combined experimental-theoretical iterative procedure. The first step is to use the measured "relative phase vs. relative thickness" data in order to find an initial approach for the thermal diffusivity from the slope of the curve. With this "rough" value of the thermal diffusivity, one can calculate the thermal diffusion length. Using a calibration measurement for the initial offset of the phase of the signal (by directly irradiating the empty sensor), one can also obtain the absolute value of the phase of the signal, and a "rough" value of the absolute sample's thickness. The next step is to use the obtained data, to locate the linear (in general $3\mu_{\mathrm{m}} - 5\mu_{\mathrm{m}}$) region of the thickness scan, and to perform a fit of the experimental data in this region, in order to obtain improved values for the thermal diffusivity and L_{mabs}. The correct value of the thermal diffusivity will be obtained by using a fitting procedure: the best fit will be selected by minimizing the relative error of thermal diffusivity found with Eq. (6), as compared to the best fit value of the linear part of the curve, with L_{mabs} as a fit parameter. The best relative error of the measurements performed with this method is better than ±0.5%.[20,29]

In Eq. (4), the amplitude of the PPE signal is the source of information. The sample's thermal diffusivity can be found from the slope of the PPE amplitude vs. $f^{1/2}$ or L_m, by following a similar procedure as in the case of the phase. Relative errors of ±0.5 ÷ ±1% were reported to be obtained from the thickness[18, 19] and ±2% from frequency scan measurements.[12] If the value of the thermal diffusivity is known, Eq. (4) offers the possibility to measure the sample's thermal effusivity, providing a calibration with a reference liquid is performed. If we denote the reference liquid by "*r*", we have for the normalized signal:[22]

$$\ln|V_n| = \ln\frac{(b_{wr}+1)(b_{rp}+1)}{(b_{wm}+1)(b_{mp}+1)} - L_m(a_r - a_m) \tag{7}$$

If "y_0" is the value of the free term in Eq. (7), we obtain for the sample's thermal effusivity e_m the following equation:

$$e_p^{-1}e_m^2 + \left[\left(1+e_w e_p^{-1}\right) - 2|V_n|^{-1}\left(1+e_r e_p^{-1}\right)\exp\left(-y_0\right)\right]e_m + e_w = 0 \tag{8}$$

The maximum reported relative error of the investigations performed with this method is of about ±2%,[22] when a thickness scan is performed and about ±10% when the frequency scan technique is used.[22, 12]

2. 2. Front Configuration

In order to deduce the theoretical equations for the particular detection cases in the front configuration, we consider the same geometry as in Fig. 1, but without the material layer, "*m*". In this case, the front opaque electrical contact of the sensor is directly irradiated, and the substrate "*s*" plays the role of sample. With the same restrictions of thermally thick window and substrate, the PPE voltage is given by:[1, 5, 23]

$$V = \frac{V_0}{(b_{wp}+1)}\frac{1 - e^{-\sigma_p L_p} + R_{sp}(e^{-2\sigma_p L_p} - e^{-\sigma_p L_p})}{1 - R_{wp}R_{sp}e^{-2\sigma_p L_p}} \tag{9}$$

As in the case of the back configuration, in order to eliminate the instrumental factor V_0, a normalization procedure is necessary. The best reference signal is obtained with air instead of substrate. Assuming that $R_{sp} = R_{gp} = -1$, one gets for the normalized signal:

$$V_n = 1 - (1+R_{sp})e^{-\sigma_p L_p} \tag{10}$$

If we extract the phase and amplitude from Eq. (10) we obtain for the phase:

$$\Theta = \arctan\frac{(1+R_{sp})\sin(a_p L_p)e^{-a_p L_p}}{1-(1+R_{sp})\cos(a_p L_p)e^{-a_p L_p}} \tag{11}$$

and for the amplitude:

$$|V_n| = \left\{ \left[(1+R_{sp}) \sin(a_p L_p) e^{-a_p L_p} \right]^2 + \left[1 - (1+R_{sp}) \cos(a_p L_p) e^{-a_p L_p} \right]^2 \right\}^{1/2} \quad (12)$$

If the expression for the amplitude seems to be rather complicated in this case for direct experimental measurements, the phase of the PPE signal can be easily used in order to obtain the sample's (substrate in this case) thermal effusivity. From Eq. (10) R_{sp} can be derived as:

$$R_{sp} = \frac{\tan\Theta}{\left[\sin(a_p L_p) + \cos(a_p L_p)\tan\Theta\right] e^{-a_p L_p}} - 1 \quad (13)$$

and the sample's thermal effusivity as:

$$e_s = e_p \frac{1+R_{sp}}{1-R_{sp}} \quad (14)$$

In fact, one performs in practice a frequency scan of the phase of the signal and one finds the thermal effusivity by optimizing the fit performed on the experimental data with Eq. (12), with e_s as a fit parameter. The method leads to measurements with ±1% relative error.

In this configuration, the amplitude was used (in the thermally thin regime for the sensor) for obtaining single values of sample's thermal effusivity,[8,9,24] but during last years, it was used mainly for getting information about the pyroelectric sensor's thermal properties.[25–27]

Table 1 contains a synthesis of the particular cases, based on scanning procedures, developed until now for PPE measurement of dynamic thermal parameters.

3. Experimental

3. 1. Experimental Set-up

The experimental set-up for PPE calorimetry contains some typical components (Fig. 2).[6,13,15,18]

The radiation source, usually a laser, is modulated by an acousto-optical modulator or an electro-mechanical chopper. The PPE signal is processed with a lock-in amplifier. A computer, provided with adequate software, is used for data acquisition. When necessary, a thermostat, provided with Peltier elements,[27] or "cold finger" refrigerator systems[6] with additional equipment (programmable

Table 1. PPE particular cases (based on scanning procedures) for the measurement of dynamic thermal parameters.

detection configuration	source of information	parameter to be scanned	thermal parameter (best reported relative error)
back	amplitude	chopping frequency	diffusivity (±2%)[12] effusivity (±10%)[12]
	amplitude	sample's thickness	diffusivity (±0.5%)[18, 19] effusivity (±2%)[22]
	phase	chopping frequency	diffusivity (±2%)[12]
	phase	sample's thickness	diffusivity (±0.5%)[11, 14, 19–21]
front	phase	chopping frequency	effusivity (±1%)[23, 28]

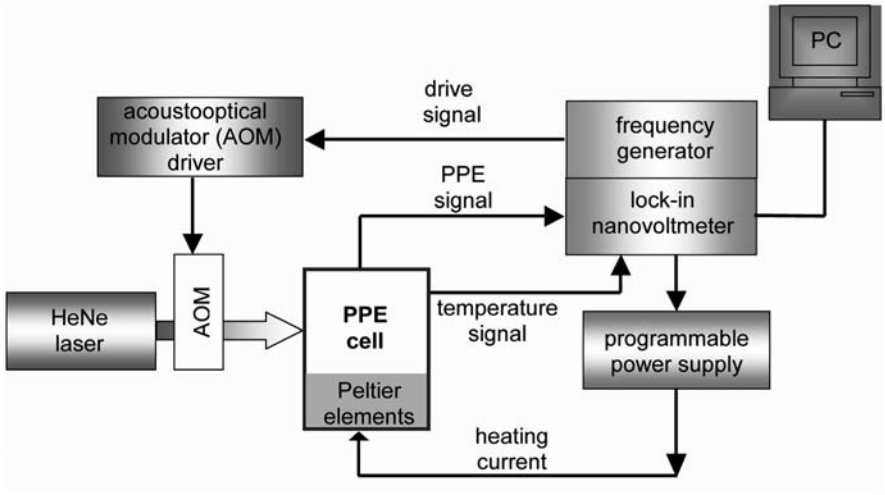

Figure 2. Typical experimental set-up for PPE calorimetry.

power supply, electronic thermometer, etc.) for temperature control, is included in the set-up.[13,15,18]

3. 2. Detection Cells

In the front configuration, usually, the space between the sensor and a glass window accommodates the liquid sample, its thickness being delimitated by two glass spacers. Sometimes, the sample simply fills a cylinder glued on the rear side of the sensor. The sample's thickness is rather large (3–5 mm, depending on the chopping frequency), in order to assure the thermally thick regime for the sample. $LiTaO_3$ and PVDF pyroelectric sensors were both used in experiments, but $LiTaO_3$ seems to be more suitable due to its rigidity. It is important to point out that the cell's design must allow to fill it and remove the sample without moving the sensor. The optical opacity of the sensor was always ensured by its front electrode.

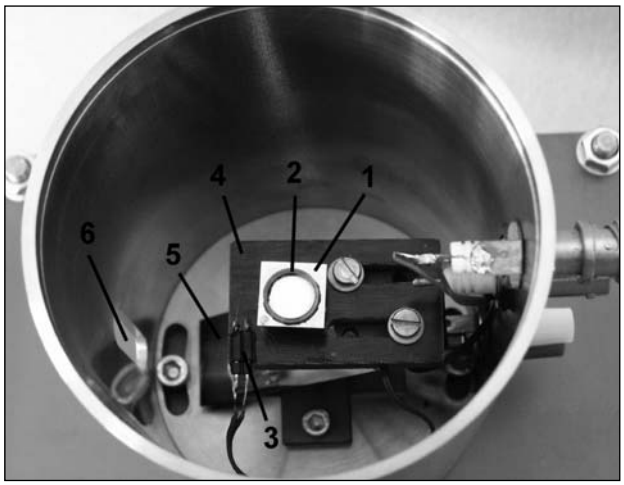

Figure 3. Image of the front detection cell presently used by the authors (1 – $LiTaO_3$ sensor; 2 – cylindrical sample holder; 3 – electrical contacts; 4 – insulating table; 5 – mirror; 6 – slot for incident laser radiation).

An image of the front detection cell presently used by the authors is displayed in Fig. 3.

Many types of detection cells were designed for the back configuration,[6,27] depending on the purpose of the experiment. We will present here an alternative one, proposed by the authors for investigations by thickness scan method (Fig. 4).[15]

The cell is based on two micrometer systems, one (with a precision of 5 μm) that performs the sample's thickness scan by modifying the distance between the sensor and an irradiated (50 μm thick) Be foil, and the other (with a precision of 1 μm) for a rigorous control of the thickness variation. The liquid sample fills the space between the sensor, the Be foil and a plastic ring, glued on the sensor with silicon rubber. As stated above, the precision in the thickness variation control offered by this cell is of about 1 μm.

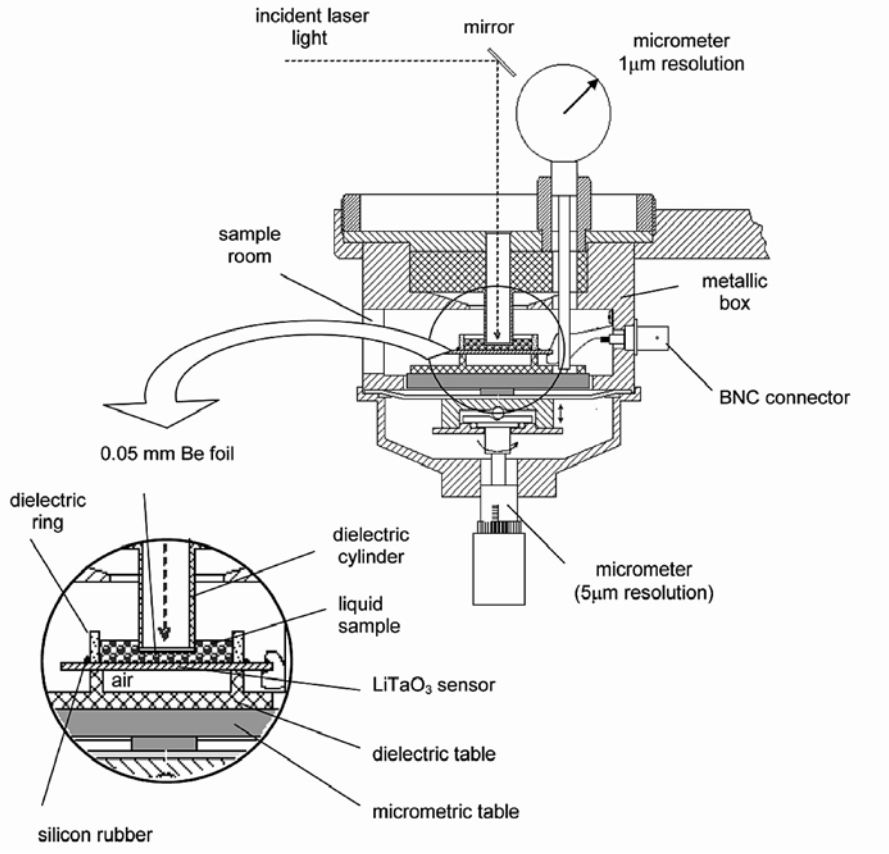

Figure 4. Schematic diagram of a two-micrometric-system back configuration cell.

For high resolution measurements, required by molecular and/or isotopic association studies in liquid mixtures, this resolution proved to be not always enough.[28, 29] Consequently, new detection cells, based on motors with nanometer resolution, were designed. An image of the cell, presently used by the authors, is displayed in Fig. 5.

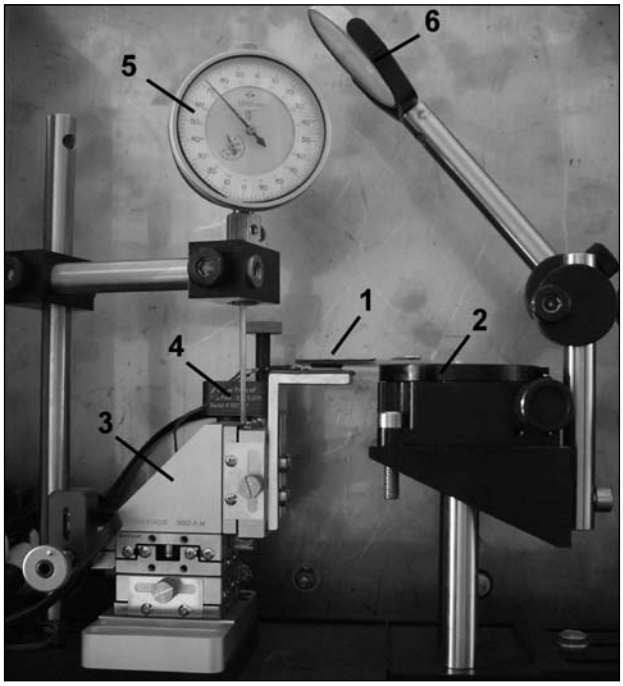

Figure 5. Image of the back detection cell presently used by the authors (30 nm step thickness control): 1 – PPE cell; 2 – rotating table; 3 – XYZ motion control system; 4 – motor with nanometer resolution for vertical motion control; 5 – micrometer; 6 – mirror reflecting the incident laser radiation.

The pyroelectric sensor, a 500 μm thick $LiTaO_3$ single crystal, provided with Cr–Au electrodes on both faces, was glued on a micrometric table. The backing material for the sensor is air. The modulated radiation passes through a 1.2 mm thick quartz window, situated on a rotating table, and is absorbed by an opaque 0.1 μm thick titanium layer, deposited on the rear side of the window. The space between the sensor and the titanium layer accommodates the liquid sample. The sample's thickness variation is performed with a step of 0.03 μm (9062M-XYZ-PPP Gothic-Arch-Bearing Picomotor).

This cell is now successfully used for thermal diffusivity measurements of magnetic nanofluids.[30]

Other solutions for back detection cells, specially designed for calorimetric investigations in the TWRC configuration, can be found in Mandelis and Matvienko.[11]

4. Applications

In this chapter, we will present some recent applications of the PPE calorimetry of liquids. The applications, performed during last years by the authors, refer to liquids of large interest: isotopic liquid mixtures, liquid foodstuffs, magnetic nanofluids. The applications stress especially on high resolution measurements of room temperature values of dynamic thermal parameters.

The temperature dependence of the thermal parameters and associated processes as phase transitions, for example, are ignored. "Classical" applications in which the thermal diffusivity and effusivity were obtained in the back (standard) detection configuration, by performing a frequency scan of the PPE amplitude and phase, were largely used in the past; consequently, they are well known and ignored in this paper too.

We intend in fact to prove that *the high resolution PPE calorimetry* can be used in order to obtain information about intimate processes in liquids, as molecular associations, compositional changes in ferrofluids, early spoilage of vegetable oils, etc. It is important that this information is obtained through the values of macroscopic (dynamic thermal parameters) and not microscopic parameters, but only provided *high resolution measurements* are performed.

4. 1. Isotopic Liquid Mixtures

In principle, concerning molecular association processes in binary mixtures, the liquids are divided in two classes: "interacting" and "non-interacting" liquids.[15,16] When interacting liquids are involved in a binary mixture (water-ethanol, for example), large deviations from additivity for all thermal parameters were found. In the case of non-interacting liquids (water- ethylene glycol, for example), the excess values (deviation from linearity) of the thermal parameters are small (few percents) or zero.

In such a context, a PPE calorimetry applied to isotopic liquid mixtures represents a challenge; small deviations from linearity of the thermal parameters as a func-

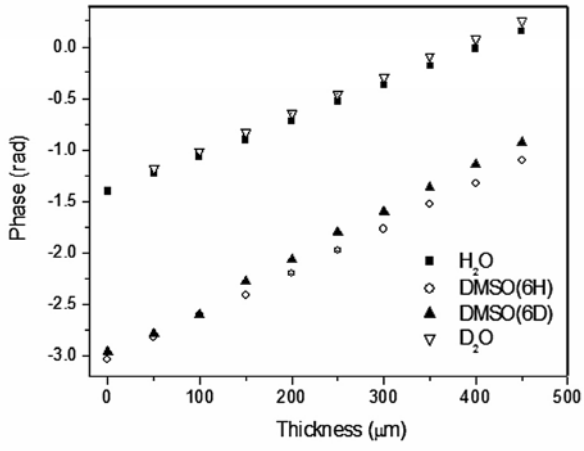

Figure 6. Typical thickness scans of the phase of the PPE signal, in the back configuration, for the pure components of the investigated isotopic mixtures.

tion of composition are expected and, consequently, accurate investigations are necessary.

Mixtures of H_2O–D_2O and of two isotopic dimethylsulfoxide species, C_2H_6OS and C_2D_6OS (denoted by DMSO(6H) and DMSO(6D)), were selected for investigations.

The thermal diffusivity was measured in the back configuration, sample's thickness scan method,[20,21] and the thermal effusivity, in the front configuration, by making use of a frequency scan of the phase of the signal.[23]

Typical thickness scans of the phase of the PPE signal, in the back configuration, for pure H_2O, D_2O, DMSO(6H) and DMSO(6D) are presented in Fig. 6.

The corresponding frequency scans of the normalized phase, in the front configuration, are displayed in Fig. 7.

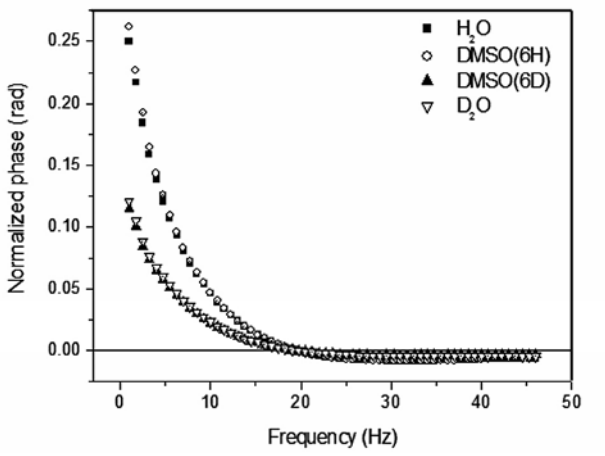

Figure 7. Typical frequency scans of the phase of the PPE signal, in the front configuration, for the pure components of the investigated isotopic mixtures.

The obtained relative deviations from additivity for the thermal diffusivity and effusivity for H_2O–D_2O, DMSO(6H)–DMSO(6D) and H_2O–DMSO(6H) are presented in Figs. 8 and 9, respectively.

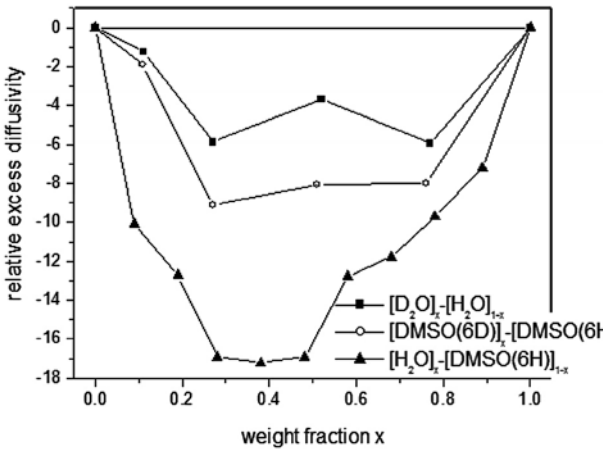

Figure 8. Relative deviations from additivity of the thermal diffusivity for H_2O–D_2O and DMSO(6H)–DMSO(6D), together with a mixture (H_2O–DMSO(6H)) known for its "aggressivity" in forming molecular associations.

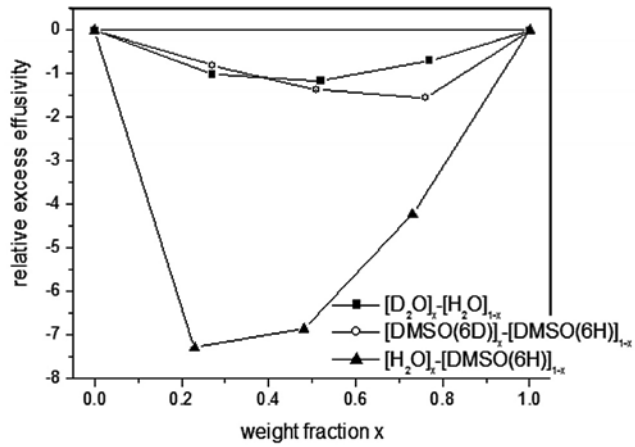

Figure 9. Relative deviations from additivity of the thermal effusivity for H_2O–D_2O and DMSO(6H)–DMSO(6D), together with a mixture (H_2O–DMSO(6H)) known for its "aggressivity" in forming molecular associations.

The maximum relative deviation from additivity of the thermal diffusivity for H_2O–DMSO(6H) mixtures is about –18% and indicates association processes taking place in this system. In fact, DMSO is well known for its hygroscopicity; this is the reason why this mixture was selected as comparison system. On the other hand, the maximum relative deviations from additivity of the thermal diffusivity for H_2O–D_2O and DMSO(6H)–DMSO(6D) are about –4% and –8%, respectively. This fact can be explained only as an isotopic effect because, from chemical point of view, H_2O and D_2O, and DMSO(6H) and DMSO(6D) molecules, respectively, are almost equivalent.

Concerning the relative deviations of the thermal effusivity, they are about –1% ÷ –2%, at the resolution limit of our method. The same deviation for H_2O–DMSO(6H) mixtures is about –7% ÷ –8%, respecting the (about) 3× reduction factor for the sensitivity (in detecting molecular associations) of thermal effusivity, as compared to thermal diffusivity, observed for water-ethanol mixtures.[16]

4. 2. Vegetable Oils

It is well known that vegetable oils have rather distinct compositions. The main fatty acid in the composition of sunflower, hemp and soybean is the linoleic acid, with about 70%, 56% and 55% concentration. In the same oils, the concentration of oleic fatty acid is around 13%–18%, the hemp and soybean oils containing rather large amounts of α-linolenic fatty acid too, about 15% and 9%, respectively. The main component in flax oil is the α–linolenic fatty acid (47%); linoleic and oleic fatty acids are present in proportion of about 20%–21%.

During a degradation process, the fatty acids composition of the vegetable oils changes. Usually, the percenta-

ge of mono and poly-unsaturated fatty acids (linoleic, α- and γ–linolenic, for example) decreases, due to their degradation, while saturated fatty acids (palmitic, stearic, oleic, etc.) are more stable and their relative concentrations increases, when determined by gas chromatography.[30]

In the following, we will present an application in which, based on accurate measurements of the thermal diffusivity, one can find a correlation between the room temperature value of the thermal diffusivity and the oils' composition.

The thermal diffusivity was measured in the back configuration, sample's thickness scan method (Fig. 10).[20, 21]

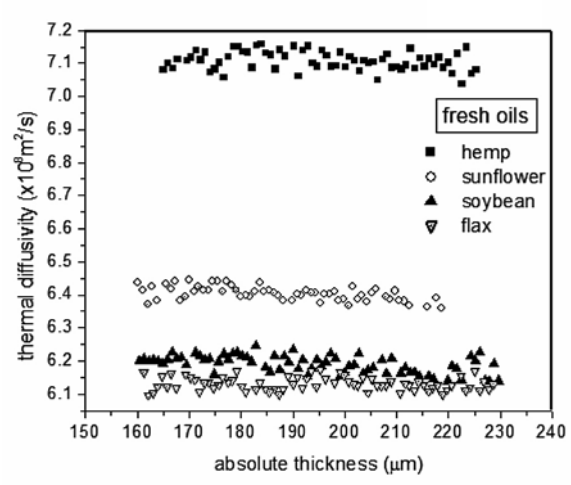

Figure 10. Thickness scan of the thermal diffusivity, in the linear region of the graph, for fresh hemp, sunflower, soybean and flax oils.

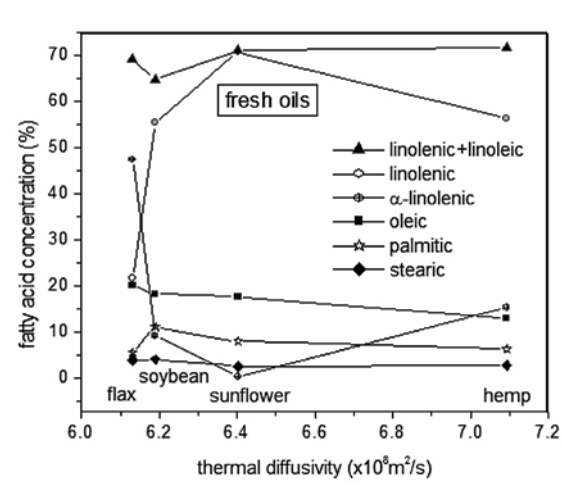

Figure 11. Thermal diffusivity vs. concentration of stearic, palmitic, oleic, α-linolenic and linoleic fatty acids, for the investigated fresh oils.

Fig. 11 presents the behaviour of thermal diffusivity as a function of main fatty acids composition (obtained by gas-chromatography) of some fresh vegetable oils. The only possible correlation can be established between the values of the thermal diffusivity and the percentage of the total amount (linoleic plus linolenic) of unsaturated fatty acids; the total amount of the above-mentioned fatty acids slightly decreases with decreasing thermal diffusivity.

Fig. 12 presents the correlation of the thermal diffusivity with the composition of hemp oil degraded in microwaves field for 6, 28 and 40 min. The same correlation with the total amount of unsaturated fatty acids was found. It is to be mentioned that the value of the thermal diffusivity does not depend on the saturated fatty acids (oleic, palmitic and stearic) composition. The relative error of the measurements is of about ±0.5%.

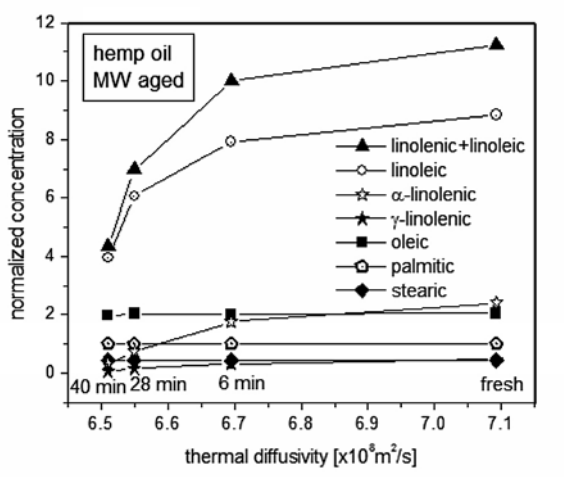

Figure 12. Normalized concentration (palmitic acid as internal standard) vs. thermal diffusivity for the main fatty acids composing hemp oil, fresh and exposed for 6, 28 and 40 min. to microwave field.

Fig 13 presents an application of the PPE calorimetry for the measurement of thermal effusivity of olive and sunflower oil. The configuration used was the back one, based on the sample's thickness scan (Eqs. (9), (10)).[22]

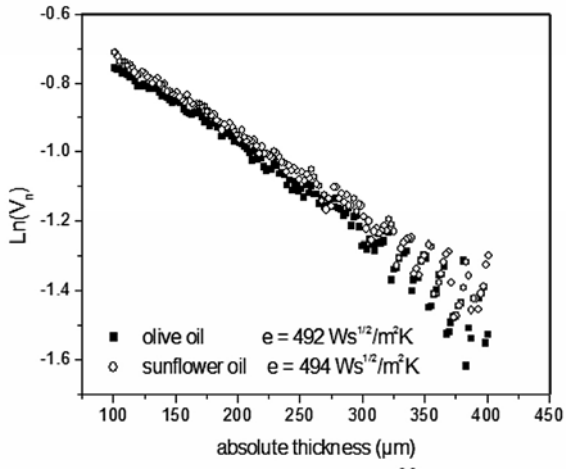

Figure 13. Thickness scan of the logarithm of the normalized amplitude for olive and sunflower oils.

This method needs two normalization procedures: one with water as reference liquid, in order to eliminate some instrumental factor, and a second one with empty sensor, directly illuminated, for finding the absolute value of the phase (and consequently, the absolute sample's thickness) of the PPE signal. The relative error of the measurements is about ±2%.

4. 3. Magnetic Nanofluids

Ferrofluids represent a special category of smart nanomaterials, consisting of stable dispersions of magnetic nanoparticles in different liquid carriers. While the magnetic properties of the magnetic nanofluids are the subject of an intensive study, there are rather few data in literature concerning their thermal properties.[31] Normally, the thermal properties of the magnetic nanofluids are expected to depend on the composition of the nanofluid (type of nanoparticles, surfactant and carrier fluid), concentration, nanoparticles' size, etc. Moreover, the values of the static and dynamic thermal parameters and their temperature behaviour (phase transitions, for example) are correlated with structural changes and/or with the dynamics of various processes (drug delivery, for example) occurring inside the nanofluid.

On the other side, the few calorimetric data from literature indicate sometimes drastic changes of the thermal conductivity of nanofluids as a function of nanoparticles' size – case of Cu nanoparticles or carbon nanotubes immersed in ethylene glycol, for example.[32,33]

In this paper we will present some accurate thermal diffusivity and effusivity measurements obtained for nanofluids based on Fe_3O_4 nanoparticles.

The thermal diffusivity was measured in the back configuration, by making use of the sample's thickness scan.[20,21]

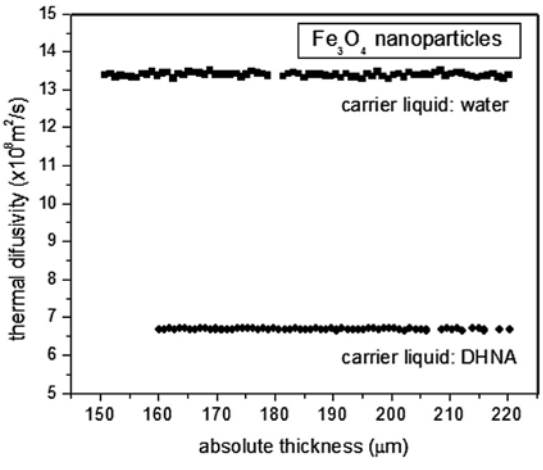

Figure 14. Typical thickness scans of the thermal diffusivity, in the thermally thick regime for the sample, for nanofluids with Fe_3O_4 nanoparticles stabilized with double layer of oleic acid, in different carrier liquids: water and DHNA, respectively.

Fig. 14 presents the thickness scan of the thermal diffusivity, obtained for nanofluids based on Fe_3O_4 nanoparticles stabilized by a double layer of oleic acid, with different carrier fluid, water and decahydronaphtalene (DHNA), respectively.

Fig. 15 displays thickness scans of the thermal diffusivity for water-based nanofluids with different concentrations of Fe_3O_4 nanoparticles.

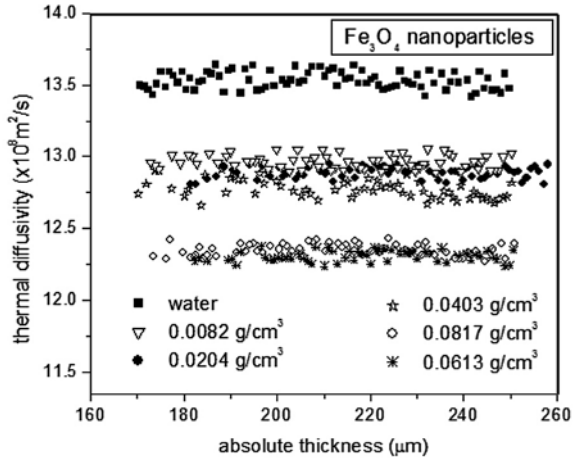

Figure 15. Results of the thickness scans obtained for the thermal diffusivity for water-based nanofluids with Fe_3O_4 nanoparticles at different concentration.

Figs. 14 and 15 indicate that thermal diffusivity is a sensitive thermal parameter to changes of main nanofluids' parameters (carrier liquid, type and concentration of nanoparticles). The relative error of the measurements was better than ± 0.5%.

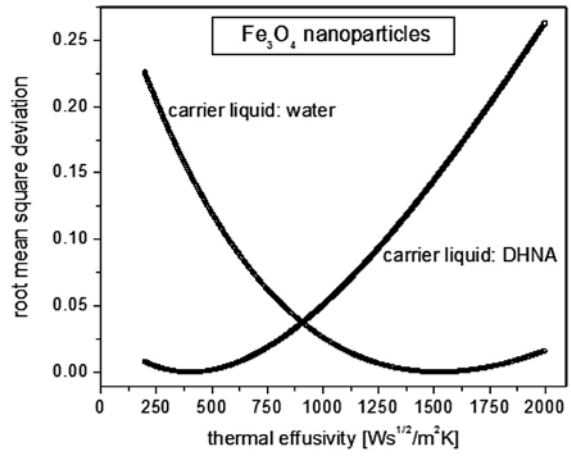

Figure 16. Root mean square deviation of the fit performed with Eq. (14) on the experimental data (PPE phase as a function of chopping frequency), with sample's thermal effusivity as a fit parameter. The minimum of the curve indicates the correct value of the thermal effusivity. Sample: nanofluid with Fe_3O_4 nanoparticles and different liquid carrier (water and DHNA, respectively).

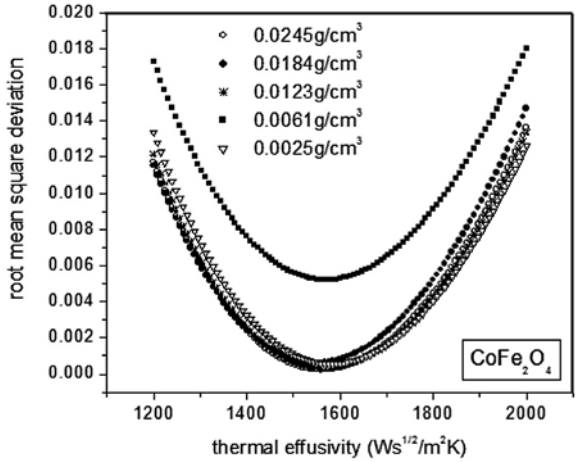

Figure 17. Root mean square deviation of the fit performed with Eq. (14) on the experimental data (PPE phase as a function of chopping frequency), with sample's thermal effusivity as a fit parameter. The minimum of the curve indicates the correct value of the thermal effusivity. Sample: water-based nanofluid with Fe_3O_4 nanoparticles.

The thermal effusivity was measured in the front configuration, by making use of a frequency scan (method proposed in ref. 23).

Figs. 16 and 17 present the optimization of the fits performed in order to calculate the thermal effusivity. The same nanofluid samples were used for investigations. The correct value of the thermal effusivity minimizes the root mean square deviation of the fit performed with Eq. (14).

As one can see, the thermal effusivity depends also on the main parameters of the nanofluid, but it is less sensitive than thermal diffusivity. The changes of the thermal effusivity as a function of liquid carrier are clearly detected, but the changes as a function of type of nanoparticles and concentration lie somewhere within the relative error of the measurement (±1%).

5. Conclusions

A review of the main PPE calorimetric techniques dedicated to high resolution measurements of dynamic thermal parameters (thermal diffusivity and effusivity) of liquids was presented.

Several combinations of experimental parameters (detection configuration, "scanning" parameters, source of information, method of data processing), optimized in order to improve the accuracy of the results, were described.

Concerning the detection configuration, the "back" one was more exploited. All the possible combinations "source of information – scanning parameter" were used in order to measure both thermal diffusivity and effusivity. The "front" configuration was used until now only with the chopping frequency as scanning parameter and only the thermal effusivity resulted from the measurements. We consider that a detection scheme based on sample's thickness scan can be also designed (small changes in the experimental set-up are necessary), but it is less probable that it can bring some improvements from accuracy point of view. Such a detection scheme is probably similar to that proposed by S. Pittois et al.,[34] low chopping frequencies and limited thickness scan range being required.

The competition between PPE "amplitude" and "phase" as source of information seems to be won by the second one, even if both lead sometimes to the same resolution of the measurement. It is more convenient to measure the phase of the signal, because the phase represents only a time delay of the signal, as compared to a reference one, and it is not dependent on the power fluctuations of the incident radiation and on the quality of the incident surface (as is the case of the amplitude). Consequently, high signal/noise ratios are expected.

As stated above, many detection schemes were proposed in the past for investigating the thermal parameters of condensed matter samples, but most of them were based on measurements of single values (fixed chopping frequency and sample's thickness). Well known are, for example, the methods using the front configuration, with opaque or semi-transparent sensor, for thermal effusivity measurement.[8,9] During last years, the scanning procedures proved to be much more accurate. In the case of liquid samples, two experimental parameters can be scanned: the chopping frequency and the sample's thickness. Both lead to accurate values for thermal parameters. A special attention has to be paid to the new developed TWRC schemes. This detection method, combined with a small enough thickness variation step and with an adequate procedure for data analysis, can lead to high accuracy for thermal diffusivity data.[11,20,21]

Concerning the "targets" of the measurements, both thermal diffusivity and effusivity can be obtained using the PPE amplitude and phase as source of information. If, in a thermal effusivity measurement, at least one calibration procedure is involved, a normalization technique is not always necessary when thermal diffusivity measurements are performed. The case when the thermal diffusivity is deduced from the slope of the phase as a function of $f^{½}$, or as a function of sample's thickness, is an example when no calibration is required. In many cases, the measurement of the thermal effusivity is conditioned by the knowledge of thermal diffusivity.[22] The final resolution is always better in the case of thermal diffusivity.

As mentioned in introduction, the four thermal parameters are connected by two relationships; the direct measurement of two of them leads automatically to the possibility of calculating the remaining two (thermal conductivity and volume specific heat). In fact, thermal conductivity and specific heat can be also directly measured with the PPE technique,[34] but this was not the purpose of the present paper.

The area of applications described in this review refers to "special" type of liquid samples, as nanofluids or isotopic liquid mixtures, where the high resolution and small quantity of sample required are clear advantages of the PPE technique, as compared to classical calorimetry.

One of the purposes of this paper was to demonstrate that intimate processes occurring in liquid samples, as molecular and isotopic associations, compositional changes in nanofluids and/or vegetable oils, can be studied by PPE calorimetry, provided accurate measurements are performed. In fact, the high-resolution PPE calorimetry is able to investigate any process associated with small changes in the dynamic thermal parameters.

The growing interest in PPE calorimetric investigations of liquids is not only due to their high sensitivity, stability and reproducibility, but also to the simplicity of the detection cells and laboratory instrumentation involved.

6. Acknowledgements

The authors wish to thank Prof. A. Mandelis for offering the possibility to access the galley proofs.[11]

Work supported by the Romanian Ministry of Education and Research through the National Research Programs CEEX 65/2006 and 39N/2006.

7. References

1. A. Mandelis, *Chem. Phys. Lett.* **1984**, *108*, 388–391.
2. D. Dadarlat, M. Chirtoc, R. M. Candea, I. Bratu, *Infrared Phys.* **1984**, *24*, 469–471.
3. H. Coufal, *Appl. Phys. Lett.* **1984,** *44*, 59–61.
4. A. Mandelis, M. M. Zver, *J. Appl. Phys.* **1985,** *57*, 4421–4431.
5. M. Chirtoc, G. Mihailescu, *Phys. Rev.* **1989,** *B40*, 9606–9617.
6. D. Dadarlat, D. Bicanic, H. Visser, F. Mercuri, A. Frandas, *J. Amer. Oil Chem. Soc.* **1995**, *72*, 273–280; *J. Amer. Oil Chem. Soc.* **1995,** *72*, 281–290.
7. M. Marinelli, F. Mercuri, U. Zammit, R. Pizzoferrato, F. Scudieri, D. Dadarlat, *Phys. Rev.* **1994,** *B49*, 9523–9532.
8. D. Dadarlat, M. Chirtoc, C. Neamtu, R. Candea, D. Bicanic, *Phys. Stat. Sol.* **1990,** *(a)121*, K231–234.
9. D. Dadarlat, A. Frandas, *Appl. Phys.* **1993,** *A56*, 235–238.
10. D. Dadarlat, H. Visser, D. Bicanic, *Meas. Sci. Technol.* **1995,** *6*, 1215–1219.
11. A. Mandelis, A. Matvienko, in: D. Remiens (Ed.): Pyroelectric Materials and Sensors, Kerala, India, **2007**, pp. 61–97.
12. S. Delenclos, M. Chirtoc, A. Hadj Sahraoui, C. Kolinsky, J. M. Buisine, *Rev. Sci. Instrum.* **2002,** *73*, 2773–2781.
13. J. Shen, A. Mandelis, *Rev. Sci. Instrum.* **1995,** *66*, 4999–5005.
14. J. Shen, A. Mandelis, H. Tsai, *Rev. Sci. Instrum.* **1998,** *69*, 197–203.
15. D. Dadarlat, C. Neamtu, E. Surducan, A. Hadj Sahraoui, S. Longuemart, D.Bicanic, *Instr. Sci. Technol.* **2002**, *30*, 387–396.
16. C. Neamtu, D. Dadarlat, M. Chirtoc, A. Hadj Sahraoui, S. Longuemart, D. Bicanic, *Instr. Sci. Technol.* **2006**, *34*, 225–234.
17. A. Sikorska, D. Dadarlat, B.B.J. Linde, M. Streza, C. Neamtu, A. Sliwinski, *J. Physique IV*, **2006,** *137*, 341–345.
18. J. A. Balderas-Lopez, A. Mandelis, J. A. Garcia, *Rev. Sci. Instrum.* **2000**, *71*, 2933–2937.
19. J. A. Balderas-Lopez, A. Mandelis, *Rev. Sci. Instrum.* **2003,** *74*, 700–702.
20. S. Delenclos, D. Dadarlat, N. Houriez, S. Longuermart, C. Kolinsky, A.H. Sahraoui, *Rev. Sci. Instrum.* **2007,** *78*, 024902.
21. D. Dadarlat, C. Neamtu, R. Pop, M. Marinelli, F. Mercuri, *J. Optoelectron. Adv. Mat.* **2007,** *9*, 2847–2852.
22. D. Dadarlat, C. Neamtu, N. Houriez, S. Delenclos, S. Longumart, A. H. Sahraoui, *Eur. Phys. J. Special Topics* **2008**, *153*, 115–118.
23. D. Dadarlat, C. Neamtu, *Meas. Sci. Technol.* **2006**, *17*, 3250–3254.
24. D. Dadarlat, M. Bicazan, A. Frandas, V.V Morariu, A. Pasca, H. Jalink, D. Bicanic, *Instr. Sci. Technol.* **1997**, *25*, 235–240.
25. S. Longuermart, A.H. Sahraoui, D. Dadarlat, S. Delenclos, C. Kolinsky, J. M. Buisine, *Rev. Sci. Instrum.* **2003**, *74*, 805–807.
26. A. Hadj Sahraoui, S. Longuemart, D. Dadarlat, S. Delenclos, C. Kolinsky, J. M. Buisine, *Ferroelectrics* **2003**, *289*, 97–106.
27. H. Jalink, A. Frandas, R. van der Schoor, D. Bicanic, *Rev. Sci. Instrum.* **1996**, *67*, 3990–3993.
28. D. Dadarlat, C. Neamtu, V. Tosa, M. Streza, *Acta. Chim. Slov.* **2007**, *54*, 149–153.
29. D. Dadarlat, C. Neamtu, M. Streza, D. Chicea, A. Pasca, *J. Optoelectron. Adv. Mat.* **2008**, *10*, 284–287.
30. F. Caponio, A. Pasqualone, T. Gomes, *J. Food Sci. Technol.* **2003**, *38*, 481–486.
31. P. Kebilinski, J. A. Eastman, D. G. Cahill, *Materials Today* **2005**, *8*, 36–44.
32. J. A. Eastman, S. U. S. Choi, S. Li, W. Yu, L. J. Thomson, *Appl. Phys. Lett.* **2001**, 78, 718–720.
33. S. U. S. Choi, Z. G. Zhang, W. Yu, F. E. Lockwood, E. A. Grulke, *Appl. Phys. Lett.* **2001,** *79*, 2252–2254.
34. See for example S. Pittois, M. Chirtoc, C. Glorieux, W. van den Bril, J. Thoen, *Analytical Sci. (Japan)* **2001,** *17*, S110-113 and references therein.

Povzetek

Podan je pregled najpomembnejših fotopiroelektričnih (FPE) metod v kalorimetriji, ki se v zadnjem času uporabljajo za natančne meritve dinamičnih termičnih parametrov (npr. termične efusivnosti in termične difuzivnosti) v tekočinah. Obravnavamo možnosti dveh konfiguracij detekcije v FPE (»back«, »front«), primerjamo informacije, dostopne v amplitudi ter fazi FPE signala ter natančnost dinamičnih metod. Opisano je nekaj aplikacij natančnih meritev termične difuzivnosti in efuzivnosti v nekaterih tekočinah (tekoče mešanice izotopov, magnetni nanofluidi, tekoča živila).